Chemical Engineering Journal 214 (2013) 8–16

Contents lists available at SciVerse ScienceDirect

Chemical Engineering Journal

journal homepage: www.elsevier.com/locate/cej

Application of chitosan films for the removal of food dyes from aqueous solutions by adsorption

G.L. Dotto, J.M. Moura, T.R.S. Cadaval, L.A.A. Pinto *

Unit Operation Laboratory, School of Chemistry and Food, Federal University of Rio Grande – FURG, 475 Engenheiro Alfredo Huch Street, 96203-900 Rio Grande, RS, Brazil

HIGHLIGHTS

- The adsorption of food dyes onto chitosan films was studied.
- The Redlich–Peterson model was the best to fit the equilibrium data.
- The maximum adsorption capacity was 194.6 mg g^{-1}.
- The adsorption process was spontaneous, favorable and exothermic.
- Chitosan films were easily separated from the liquid phase after the adsorption.

ARTICLE INFO

Article history:
Received 16 September 2012
Received in revised form 20 October 2012
Accepted 22 October 2012
Available online 30 October 2012

Keywords:
Acid red 18
Adsorption
Chitosan films
FD&C blue no. 2
Phase separation

ABSTRACT

Chitosan films were applied to remove acid red 18 and FD&C blue no. 2 dyes from aqueous solutions. The films were prepared by casting technique and characterized. Batch adsorption equilibrium experiments were carried out at different temperatures (298–328 K). Freundlich, Langmuir and Redlich–Peterson models were fitted to the experimental data. The thermodynamic parameters (ΔG^0, ΔH^0 and ΔS^0) were also estimated. Kinetic study was realized using pseudo-first order, pseudo-second order and Elovich models. The possible films–dyes interactions were investigated by Fourier transform infrared spectroscopy, differential scanning calorimetry and color parameters. The maximum experimental adsorption capacities were 194.6 mg g^{-1} and 154.8 mg g^{-1} for the acid red 18 and FD&C blue no. 2, respectively, obtained at 298 K. It was found that the Redlich–Peterson isotherm model presented satisfactory fit with the experimental data ($R^2 > 0.98$ and ARE < 9.00%). The adsorption process was spontaneous, favorable, exothermic, and occurred by electrostatic interactions. The Elovich model was the more appropriate to represent the adsorption kinetic data ($R^2 > 0.95$ and ARE < 5.00%). The chitosan films maintained its structure and were easily separated from the liquid phase after the adsorption process.

1. Introduction

Dyes are extensively used in food industries to improve the sensorial aspects of its products [1]. Due to losses in the process, a considerable amount of these food dyes are present in the industrial effluents [2]. Dyes are visible to human eye and therefore, a highly objectionable type of pollutant on aesthetic grounds. They also interfere with the transmission of light and upset the biological metabolism processes which cause the destruction of aquatic communities present in ecosystem [3]. Therefore, the dye-containing effluents from the food industries should be carefully treated before discharge. Several techniques have been used to treat dye-containing effluents [3–7]. Among these, adsorption with chitosan is considered an alternative eco-friendly technology in relation to the existing costly water treatment technologies due to low initial cost, ease of operation, insensitivity to toxic substances, and complete removal of dyes from dilute solutions [7–10].

Chitosan is a polysaccharide composed by polymers of glucosamine and N-acetyl glucosamine [7]. Due to the advantages, coupled with its biocompatibility and biodegradability, chitosan has been successfully used by several researchers as an adsorbent for the capture of dissolved dyes from aqueous solutions [7–16]. However, it is very difficult to remove the dyes adsorbed by chitosan from aqueous phase after the adsorption process [7]. An alternative to solve this problem is the development of chitosan based materials, which can facilitate the phase separation after adsorption [17].

Among the chitosan based materials (nanoparticles, gel beads, membranes, films, sponge, fibers or hollow fibers) [17], chitosan films are an attractive way to removal pollutants from aqueous solutions, mainly due its good mechanical properties [18–21]. Recently, chitosan films were applied for the removal of lead [18,19],

* Corresponding author. Tel.: +55 53 3233 8645; fax: +55 53 3233 8745.
E-mail addresses: guilherme_dotto@yahoo.com.br (G.L. Dotto), jaquefurg@gmail.com (J.M. Moura), titoeq@gmail.com (T.R.S. Cadaval), dqmpinto@furg.br (L.A.A. Pinto).

1385-8947/$ - see front matter © 2012 Elsevier B.V. All rights reserved.
http://dx.doi.org/10.1016/j.cej.2012.10.027

chromium [20], cooper and mercury [21] from aqueous solutions. However, there is a lack of information in the literature relative to the use of chitosan films for dye removal (especially food dyes) from aqueous solutions by adsorption.

In this work was studied the application of chitosan films to remove food dyes (acid red 18 and FD&C blue no. 2) from aqueous solutions, aiming to facilitate the phase separation after adsorption process. The chitosan films were prepared and characterized according to the mechanical proprieties, swelling degree, Fourier transform infrared spectroscopy (FT-IR), differential scanning calorimetry (DSC) and color parameters. The adsorption of food dyes by chitosan films was studied at different temperatures (298–328 K) through equilibrium isotherms, thermodynamic and kinetic analysis. The possible films–dyes interactions were investigated by FT–IR, DSC and color parameters.

2. Materials and methods

2.1. Food dyes

The food dyes (industrial grade, purity higher than 85%), acid red 18 (xanthene dye; molecular weight 879.86 g mol^{-1}; C.I. 45,430; λ_{max} = 526 nm; pK_a = 6.4) and FD&C blue no. 2 (indigoid dye; molecular weight 466.34 g mol^{-1}; C.I. 73,015; λ_{max} = 610 nm; pK_a = 12.2) were supplied by a local manufacturer (Duas Rodas Ind.) and were used without further purification. The optimized-three dimensional structural formulae of the dyes (obtained from ChemBio 3D 11.0.1 software (Cambridge Soft, USA)) are shown in Fig. 1. Distilled water was used to prepare all solutions. All reagents were of analytical-grade.

2.2. Preparation and characterization of chitosan films

Chitosan powder (deacetylation degree of 85 ± 1% and viscosity average molecular weight of 150 ± 3 kDa) was obtained from shrimp wastes (*Penaeus brasiliensis*) according to the procedures presented in our previously published works [22–24]. Chitosan films were prepared by casting technique as follows [25]: 1.5 g (dry basis) of chitosan powder was dissolved in 0.1 mol L^{-1} of acetic acid solution using moderate magnetic stirring (Marte, MAG-01H, Brazil), at room temperature for 120 min (pH was 3.5). Then the film-forming solution was centrifuged (Fanem, 206 BL, Brazil) at 5000*g* for 15 min. 50 mL of the film-forming solution was poured onto a level plexiglas plate in order to keep the total amount of polymer deposited constant. The chitosan films were obtained by solvent evaporation in an oven with air circulation at 40 ± 2 °C for about 24 h. Finally, the film samples were removed from plates and conditioned in desiccators prior to the use.

The mechanical properties (tensile strength and elongation) of chitosan films were measured using a Texture Analyzer (Stable Micro Systems, TA-XT-2i, UK) with a 50 N load cell equipped with tensile grips. For these mechanical tests, samples were cut into 25 mm (width) × 100 mm (length) strips. The testing speed for texture analysis was 2 mm s^{-1}. Films thickness was obtained from 10 measurements taken at different locations on film sample by a digital micrometer (Insize, IP54, Brazil) with 0.0010 mm of resolution [25,26].

To obtain the swelling degree, chitosan films were divided in portions (1 cm × 1 cm), weighed and placed in buffer disodium phosphate/citric acid solution (0.1 mol L^{-1}) (pH = 7.0) for predetermined periods of time (5, 10, 30, 60 and 120 min). Then, the films were removed from the medium and weighed after removal of the excess surface water using filter paper (Whatmann no. 40) [27]. These experiments were carried out at different temperatures (298, 308, 318 and 328 K), and the swelling degree was determined by Eq. (1) [18]:

$$\text{Swelling degree} = \frac{W_t - W_0}{W_0}(100) \quad (1)$$

where W_t is the weight of swollen sample at time t and W_0 the is weight of dry sample.

Fourier transform infrared spectroscopy (FT-IR) (Prestige, 21210045, Japan) was carried out in the range of 500–3500 cm^{-1} to identify the functional groups on chitosan films [28]. The heat effect on the films was evaluated by differential scanning calorimetry (DSC) (Shimadzu, DSC60, Japan). The chitosan films were packed in aluminum pans, and heated from 30 to 200 °C at heating rate of 10 °C min^{-1} under N_2 atmosphere (50 mL min^{-1}) [29].

The color of chitosan films was determined by Minolta system (Minolta Corporation, CR-300, Japan). Color was measured from three-dimensional color diagram (L^*, a^*, b^*), and the numerical values (a^*, b^*) were converted in Hue angle by Eq. (2) [30]:

$$H_{ab} = tan^{-1}\left(\frac{b^*}{a^*}\right) \quad (2)$$

where H_{ab} is the Hue angle (°).

2.3. Batch adsorption experiments

Typical batch experiments were carried out at different temperatures (298, 308, 318 and 328 K) to obtain the equilibrium curves of food dyes adsorption onto chitosan films. The other experimental conditions were selected on the basis in preliminary tests and literature [2,9–13,18]. Firstly, dye stock solutions (1.0 g L^{-1}) were prepared and the pH was adjusted to 7.0 through buffer disodium phosphate/citric acid solution (0.1 mol L^{-1}), which did not present interaction with the dyes [13]. After, 100 mL of dye solutions with different concentrations (20–100 mg L^{-1}) were prepared from stock solutions and placed in flasks. Then, 50 mg (dry basis) of chitosan film (divided in portions of 1 cm × 1 cm) were added in each dye solution [27]. The flasks were agitated at 100 rpm using a thermostated type Wagner agitator (Fanem, 315 SE, Brazil). Samples were analyzed every 8 h. The equilibrium was considered attained when the dye concentration in the liquid did not present difference between three consecutive measures [13]. The dyes concentration was determined by spectrophotometer (Biospectro, SP-22, Brazil) at 526 and 610 nm for the acid red 18 and FD&C blue no. 2, respectively. All experiments were carried out in replicate (three times for each experiment) and blanks were performed. The equilibrium adsorption capacity (q_e) was determined by following equation:

$$q_e = \frac{C_0 - C_e}{m}V \quad (3)$$

where C_0 is the initial dye concentration in liquid phase (mg L^{-1}), C_e is the equilibrium dye concentration in liquid phase (mg L^{-1}), m is amount of chitosan films (g), and V is the volume of solution (L).

2.4. Equilibrium isotherms

In order to fit the experimental equilibrium data of food dyes adsorption onto chitosan films, the Freundlich, Langmuir and Redlich–Peterson isotherm models were applied.

The Freundlich isotherm assumes that the adsorption occurs on a heterogeneous surface, and the amount that is adsorbed increases infinitely with an increase in concentration. The Freundlich isotherm is given by Eq. (4) [31]:

$$q_e = k_F C_e^{1/n_F} \quad (4)$$

where k_F is the Freundlich constant (mg g^{-1}) (mg L^{-1})$^{-1/n_F}$ and $1/n_F$ is the heterogeneity factor.

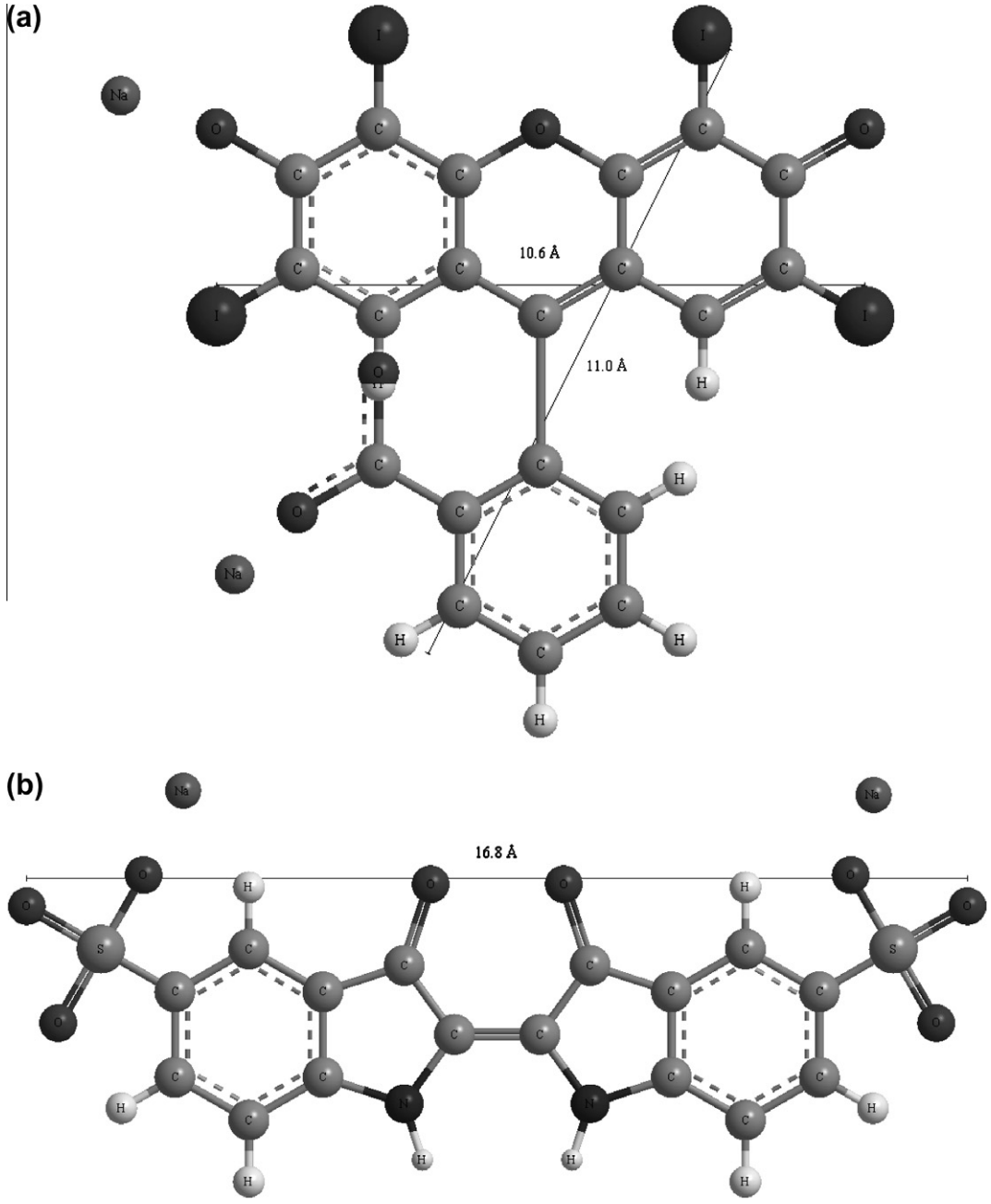

Fig. 1. Optimized three–dimensional structural formulae of the dyes: (a) acid red 18 and (b) FD&C blue no. 2.

The Langmuir isotherm model assumes a monolayer adsorption onto a homogeneous surface where the binding sites have equal affinity and energy. The Langmuir isotherm is given by Eq. (5) [32]:

$$q_e = \frac{q_m k_L C_e}{1 + (k_L C_e)} \quad (5)$$

where q_m is the maximum adsorption capacity (mg g^{-1}) and k_L is the Langmuir constant (L mg^{-1}).

Another essential characteristic of the Langmuir isotherm can be expressed by the separation factor (R_L) shown in Eq. (6) [32]:

$$R_L = \frac{1}{1 + (k_L C_0)} \quad (6)$$

The Redlich–Peterson isotherm is used to represent adsorption equilibrium over a wide concentration range, and can be applied either in homogeneous or in heterogeneous systems due to its versatility. The Redlich–Peterson isotherm is given by Eq. (7) [33]:

$$q_e = \frac{k_{RP} C_e}{1 + (a_{RP} C_e^{\beta})} \quad (7)$$

where k_{RP} and a_{RP} are the Redlich–Peterson constants (L g^{-1}) and (L $mg^{-1})^{\beta}$, respectively, and β is the heterogeneity coefficient (which varies between 0 and 1).

The isotherms parameters were determined by nonlinear regression using the software Statistica 6.0 (Statsoft, USA). The objective function was Quasi-Newton. The fit quality was measured according to the coefficient of determination (R^2) and average relative error (ARE) [34].

2.5. Thermodynamic analysis

In order to analyze the adsorption thermodynamic behavior, the values of Gibbs free energy change (ΔG^0, kJ mol^{-1}), enthalpy

change (ΔH^0, kJ mol^{-1}) and entropy change (ΔS^0, kJ mol^{-1}K^{-1}) were estimated by Eqs. (8)–(10) [35,36]:

$$\Delta G^0 = -RT\ln(55.5K_D) \quad (8)$$

$$\Delta G^0 = \Delta H^0 - T\Delta S^0 \quad (9)$$

$$\ln(55.5K_D) = \frac{\Delta S^0}{R} - \frac{\Delta H^0}{RT} \quad (10)$$

where K_D is the thermodynamic equilibrium constant (L mol^{-1}), and 55.5 is the number of moles of water per liter of solution. The K_D values were estimated from the parameters of the best fit isotherm model and the molecular weight of the dyes [35,36].

2.6. Kinetic analysis

In the more appropriate temperature (determined by the equilibrium study), experiments were carried out in order to obtain kinetic data (the experiments were carried out in the same way of Section 2.3, however, aliquots were removed at 2, 4, 6, 8, 10, 15, 20, 25, 30, 40, 60, 80, 100 and 120 min). The initial dye concentration for the kinetic tests was 100 mg L^{-1} and the stirring rate 200 rpm. All experiments were carried out in replicate and blanks were performed. In order to elucidate adsorption kinetic, pseudo-first order, pseudo-second order and Elovich models were fitted to the experimental data.

The kinetic models of pseudo-first order and pseudo-second order assume that adsorption is a pseudo-chemical reaction, and the adsorption rate can be determined, respectively, for equations of pseudo-first (Eq. (11)) [37] and pseudo-second order (Eq. (12)) [38]:

$$q_t = q_1(1 - \exp(-k_1 t)) \quad (11)$$

$$q_t = \frac{t}{(1/k_2 q_2^2) + (t/q_2)} \quad (12)$$

where q_t is the adsorbate amount adsorbed at time t (mg g^{-1}), k_1 and k_2 are the rate constants of pseudo-first and pseudo-second order models, respectively, in (min^{-1}) and (g mg^{-1} min^{-1}), q_1 and q_2 are the theoretical values for the adsorption capacity (mg g^{-1}) and "t" is the time (min).

The Elovich kinetic model can be described according to the Eq. (13) [37]:

$$q_t = \frac{1}{a} ln(1 + abt) \quad (13)$$

where "a" is the initial velocity due to dq/dt with q_t = 0 (mg g^{-1} · min^{-1}) and "b" is the desorption constant of the Elovich model (g mg^{-1}).

2.7. Analysis of chitosan films–food dyes interactions

The possible films–dyes interactions were investigated by FT-IR, DSC and color parameters (procedures presented above in the Section 2.2) [28–30]. Chitosan films were analyzed before and after (experiments at 298 K) adsorption process. For the analyses after adsorption, the films were dried at room temperature.

3. Results and discussion

3.1. Chitosan films characteristics

The chitosan films were characterized according to the mechanical proprieties, thickness swelling degree (discussed in this section), FT-IR, DSC and color parameters.

From the mechanical tests, it was observed that chitosan films presented tensile strength of 28.3 ± 1.2 MPa and elongation of 63.9 ± 1.0%. These mechanical proprieties were maintained after adsorption. The film thickness was 54 ± 1 μm. According to the literature [18,23,24], it is possible to affirm that the chitosan film showed good mechanical properties, and these properties can facilitate the phase separation after the dyes adsorption.

The swelling degree of chitosan films, at different temperatures, is presented in Fig. 2. In this figure, the swelling degree reached values of 500% within 30 min, being independent of temperature. The swelling degree is important in the context of dyes adsorption, because leads to an expansion of the porous structure [7], allowing that the large dye molecules penetrate into the chitosan film. The chitosan/poly(vinyl alcohol) films prepared by Fajardo et al. [18] presented swelling degree values in the range of 200–900%.

3.2. Equilibrium studies

Fig. 3 shows the adsorption equilibrium curves onto chitosan films, at different temperatures, for acid red 18 (Fig. 3a) and FD&C blue no. 2 (Fig. 3b). The adsorption isotherm curves of both dyes can be classified as type "H" [39], indicating a great film–dyes affinity and numerous readily accessible sites. Similar equilibrium curves were obtained in the adsorption of food dyes acid yellow 6, acid yellow 23 and acid red 18 on activated carbon [40].

The adsorption capacity of food dyes onto chitosan films was increased with the temperature decrease reaching maximum values at 298 K (Fig. 3). The temperature increase causes an increase in the solubility of the dyes [7], so, the interaction forces between the dyes and the solvent become stronger than those between dyes and chitosan films. Similar behavior was found in the adsorption of FD&C red no. 40 by chitosan [13] and in the adsorption of acid blue 9 by *Spirulina platensis* [41].

Fig. 3 shows that the adsorption capacity of FD&C blue no. 2 was lower than acid red 18. This occurred probably because molecular size of FD&C blue no. 2 is higher than molecular size of acid red 18 (see Fig. 1), leading to a difficulty in dye diffusion. According to Crini and Badot [7] the smaller dye molecules are able to undertake a deeper penetration of dye into the internal pore structure of the chitosan. In addition, the pK_a (6.4) of acid red 18 is lower than pK_a (12.2) of FD&C blue no. 2, facilitating its dissociation in the anionic form, and consequently, increasing its adsorption capacity [41].

The maximum experimental adsorption capacities were 194.6 mg g^{-1} and 154.8 mg g^{-1} for the acid red 18 and FD&C blue no. 2, respectively, obtained at 298 K. Table 1 shows a comparison

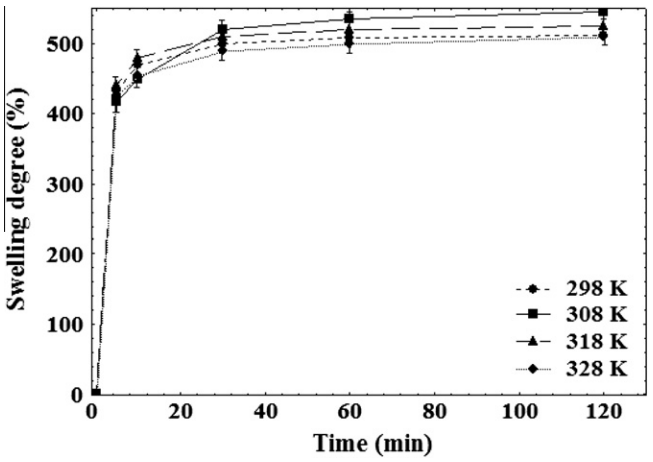

Fig. 2. Swelling degree of chitosan films at different temperatures (● 298 K; ■ 308 K; ▲ 318 K; ♦ 328 K).

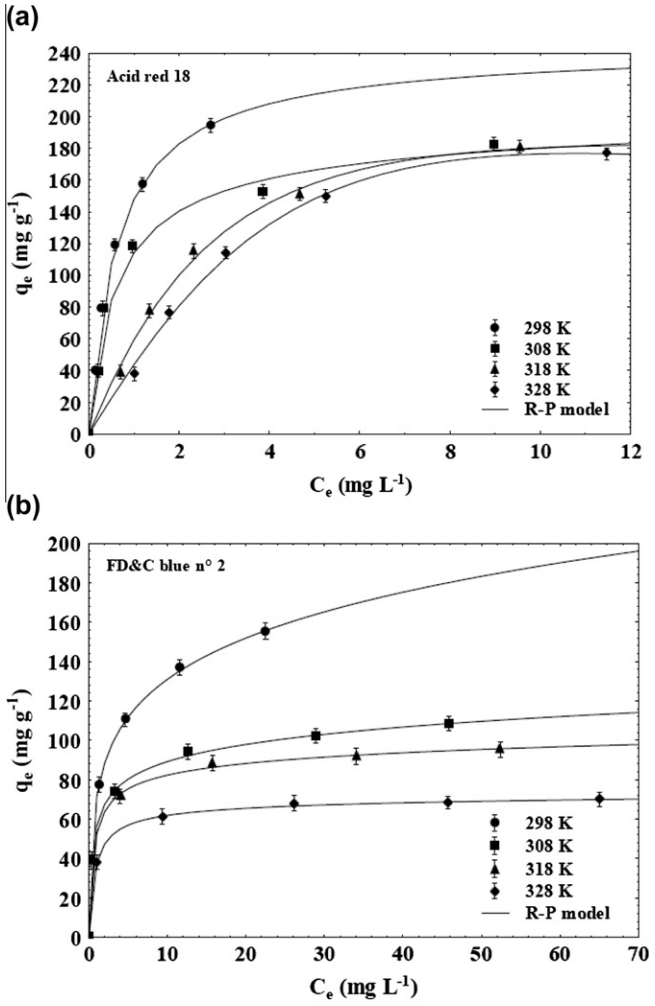

Fig. 3. Experimental adsorption equilibrium curves and Redlich–Peterson isotherm model of food dyes onto chitosan films (● 298 K; ■ 308 K; ▲ 318 K; ♦ 328 K): (a) acid red 18, and (b) FD&C blue no. 2.

between chitosan films and others adsorbents to removal food dyes. Based in Table 1, it is possible to affirm that the chitosan films presented satisfactory adsorption capacity.

To obtain information about the equilibrium data of food dyes adsorption onto chitosan films, the Freundlich, Langmuir and Redlich–Peterson isotherm models were applied. Table 2 shows the isotherm parameters for the adsorption of acid red 18 and FD&C blue no. 2 onto chitosan films at different temperatures.

The high values of coefficient of determination ($R^2 > 0.98$) and the low values of average relative error (ARE < 9.00%), presented in Table 2, show that the Redlich–Peterson model was the more adequate to fit the experimental equilibrium data. The k_{RP} parameter increased with the temperature decrease (Table 2), showing that, in the experimental range, the adsorption of food dyes onto chitosan films was favored at lower temperatures. The same dependence was found in relation to a_{RP} parameter. This shows that the film–dyes affinity was also favored at lower temperatures. Piccin et al. [13] showed that the Redlich–Peterson model was satisfactory to represent the adsorption of FD&C red no. 40 by chitosan.

3.3. Kinetic behavior

For both dyes, the adsorption kinetic curves were obtained at 298 K, 200 rpm, and initial dye concentration of 100 mg L^{-1}. Fig. 4 shows the adsorption kinetic curves of acid red 18 and FD&C blue no. 2 onto chitosan films. It was found that the adsorption of acid red 18 onto chitosan films was a relatively fast process, reaching about 70% of saturation in 120 min (Fig. 4). In the same way, for FD&C blue no. 2, 75% of saturation was attained in 80 min. After, the adsorption rate decreased considerably. Similar behavior was obtained by Dotto and Pinto [9] in the adsorption of acid blue 9 and food yellow 3 onto chitosan powder. They found about 85% of saturation in 60 min. Dotto et al. [12] in the adsorption of FD&C yellow no. 5 onto chitosan powder obtained about 95% of saturation in 80 min.

To obtain information about the food dyes adsorption onto chitosan films, pseudo-first order, pseudo-second order and Elovich kinetic models were fitted to the experimental data. The kinetic models constants, coefficients of determination (R^2) and average relative error (ARE) are shown in Table 3. The low values of average relative error (ARE < 5.0%) and the high values of coefficients of determination ($R^2 > 0.95$) (Table 3) showed that the Elovich model was the more appropriate to represent adsorption kinetic of food dyes onto chitosan films. This suggests that chitosan films were covered by superficial layer of the dyes [7,9–11,37]. Similar behavior was obtained by Piccin et al. [11] in the adsorption of FD&C red no. 40 by chitosan powder.

3.4. Thermodynamic parameters

The adsorption thermodynamic parameters were estimated by Eqs. (8)–(10). The K_D values were estimated from the Redlich–Peterson parameters, as reported in the literature [35,36]. The values of ΔG^0, ΔH^0 and ΔS^0 in all experimental conditions are show in Table 4.

The negative values of ΔG^0 (Table 4) indicate that the adsorption of food dyes onto chitosan films was a spontaneous and favorable process, whereby no energy input from outside of the system is required. Negative ΔH^0 values confirm the exothermic nature of the adsorption process. For the acid red 18 dye, the negative value of ΔS^0 indicates that randomness decreases at the solid–solution interface during the adsorption. The positive value of ΔS^0 shows

Table 1
Comparison between chitosan films and others adsorbents to removal food dyes.

Adsorbent	Food dye	Adsorbent dosage (mg L^{-1})	Dye concentration (mg L^{-1})	Adsorption capacity (mg g^{-1})	Reference
Chitosan films	Acid red 18	500	20–100	194.6	This work
Chitosan films	FD&C blue no. 2	500	20–100	154.8	This work
Chitosan powder	Acid blue 9	250	100	210.0	[10]
Chitosan powder	Food yellow 3	250	100	295.0	[10]
Chitosan powder	FD&C yellow no. 5	250	100	350.0	[12]
Chitin	FD&C yellow no. 5	250	100	30.0	[12]
Chitosan powder	FD&C red no. 40	250	20–400	529.0	[13]
Activated carbon	Acid yellow 6	1000	100–1000	673.7	[40]
Activated carbon	Acid yellow 23	1000	100–1000	643.0	[40]
Activated carbon	Acid red 18	1000	100–1000	551.8	[40]

Table 2
Isotherm parameters for the adsorption of acid red 18 and FD&C blue no. 2 onto chitosan films at different temperatures.

Temperature (K)	Acid red 18				FD&C blue no. 2			
	298	308	318	328	298	308	318	328
Isotherm model								
Freundlich								
k_F (mg g^{-1}) (mg L^{-1})$^{-1/n_F}$	134.1	99.8	68.5	60.0	69.3	55.1	52.2	41.6
n_F	2.37	3.45	2.21	2.13	3.74	5.41	6.13	7.46
R^2	0.971	0.950	0.961	0.948	0.993	0.987	0.978	0.985
ARE (%)	12.14	16.38	13.70	15.40	5.45	5.58	6.71	4.76
Langmuir								
q_m (mg g^{-1})	239.0	187.5	237.4	243.7	153.3	103.2	92.9	69.4
k_L (L mg^{-1})	1.63	1.64	0.36	0.26	0.81	1.23	1.31	1.13
R_L	0.006	0.006	0.027	0.037	0.012	0.009	0.008	0.009
R^2	0.998	0.979	0.992	0.986	0.974	0.977	0.990	0.977
ARE (%)	3.58	10.47	6.12	8.35	9.58	6.96	3.81	1.42
Redlich–Peterson								
k_{RP} (L g^{-1})	396.0	344.1	85.2	64.3	411.1	272.4	183.8	97.8
a_{RP} (L mg^{-1})$^{\beta}$	2.01	1.67	0.36	0.27	4.75	3.83	2.51	1.61
β	0.99	0.95	1.00	0.99	0.80	0.89	0.93	0.96
R^2	0.998	0.989	0.992	0.986	0.999	0.999	0.998	0.999
ARE (%)	3.33	4.71	6.12	8.45	0.64	1.01	1.06	0.53

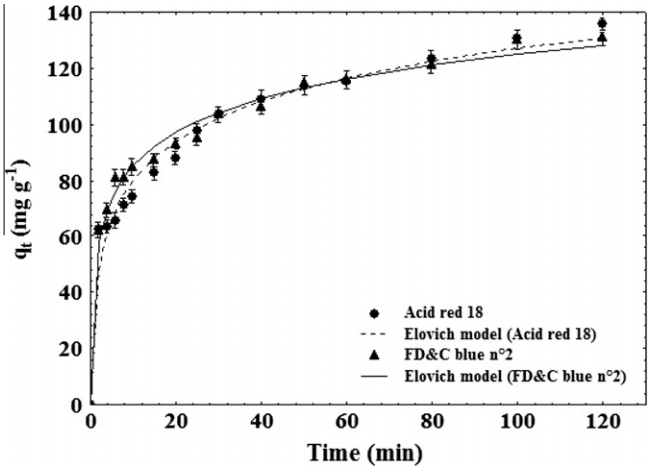

Fig. 4. Kinetic curves of the food dyes adsorption onto chitosan films (T = 298 K, 200 rpm, initial dye concentration 100 mg L^{-1}).

Table 3
Kinetic parameters for the adsorption of acid red 18 and FD&C blue no. 2 onto chitosan films.

Kinetic model	Dye	
	Acid red 18	FD&C blue no. 2
Pseudo-first order		
q_1 (mg g^{-1})	114.79	110.30
k_1 (min^{-1})	0.1279	0.2119
R^2	0.809	0.824
ARE (%)	13.01	11.73
Pseudo-second order		
q_2 (mg g^{-1})	126.94	120.92
k_2 (g mg^{-1} min^{-1})	0.0015	0.0024
R^2	0.906	0.923
ARE (%)	8.92	7.66
Elovich		
a (mg g^{-1} min^{-1})	0.0485	0.0579
b (g mg^{-1})	97.59	239.33
R^2	0.957	0.974
ARE (%)	4.39	2.58

a high preference of FD&C blue no. 2 molecules by the surface of chitosan films [35]. Furthermore, it was observed that enthalpy change (ΔH^0) contributed more than entropy change (ΔS^0) to obtain negative values of ΔG^0. This shows that the food dyes adsorption onto chitosan films was an enthalpy-controlled process. Similar thermodynamic behavior was found by others researches [41–43].

3.5. Interactions chitosan films–food dyes

The possible films–dyes interactions were investigated by FT-IR, DSC and color parameters. Fig. 5 shows the FT-IR spectrum of chitosan films: (a) before adsorption process, (b) adsorbed with acid red 18, and (c) adsorbed with FD&C blue no. 2.

In Fig. 5a, for the films before adsorption process, the major intense bands were: 3350, 3150, 2900, 2800, 1700, 1650, 1550, 1400, 1350, 1250, 1075, 1000 and 680 cm^{-1}. The peaks in the range of 3350–3150 cm^{-1} are relative to the N—H and O—H stretching. The C—H stretching can be observed at 2900–2800 cm^{-1}. Stretching vibrations of C=O and C=C were observed at 1700 and 1650 cm^{-1}, respectively. At 1550 and 1075 cm^{-1} C—N stretching vibrations of amide and amine were identified. The peaks 1400, 1350, 1250 cm^{-1} can be attributed to the CH_2 bend and C—C stretching, respectively. The band of 1000 cm^{-1} could be assigned to a C—O stretching. The N—H bending was observed at 680 cm^{-1}. All the identified peaks are common for chitosan films [18–20].

Table 4
Thermodynamic parameters for the adsorption of acid red 18 and FD&C blue no. 2 onto chitosan films.

Dye	Temperature (K)	ΔG^0 (kJ mol^{-1})	ΔH^0 (kJ mol^{-1})	ΔS^0 (J mol^{-1} K^{-1})
Acid red 18	298	−45.6 ± 0.3	−61.3 ± 0.4	−51.27 ± 0.9
	308	−46.6 ± 0.1		
	318	−44.1 ± 0.2		
	328	−44.7 ± 0.2		
FD&C blue no. 2	298	−40.4 ± 0.2	−31.4 ± 0.5	36.00 ± 1.1
	308	−41.2 ± 0.3		
	318	−41.4 ± 0.1		
	328	−41.5 ± 0.1		

Mean ± standard error (n = 3).

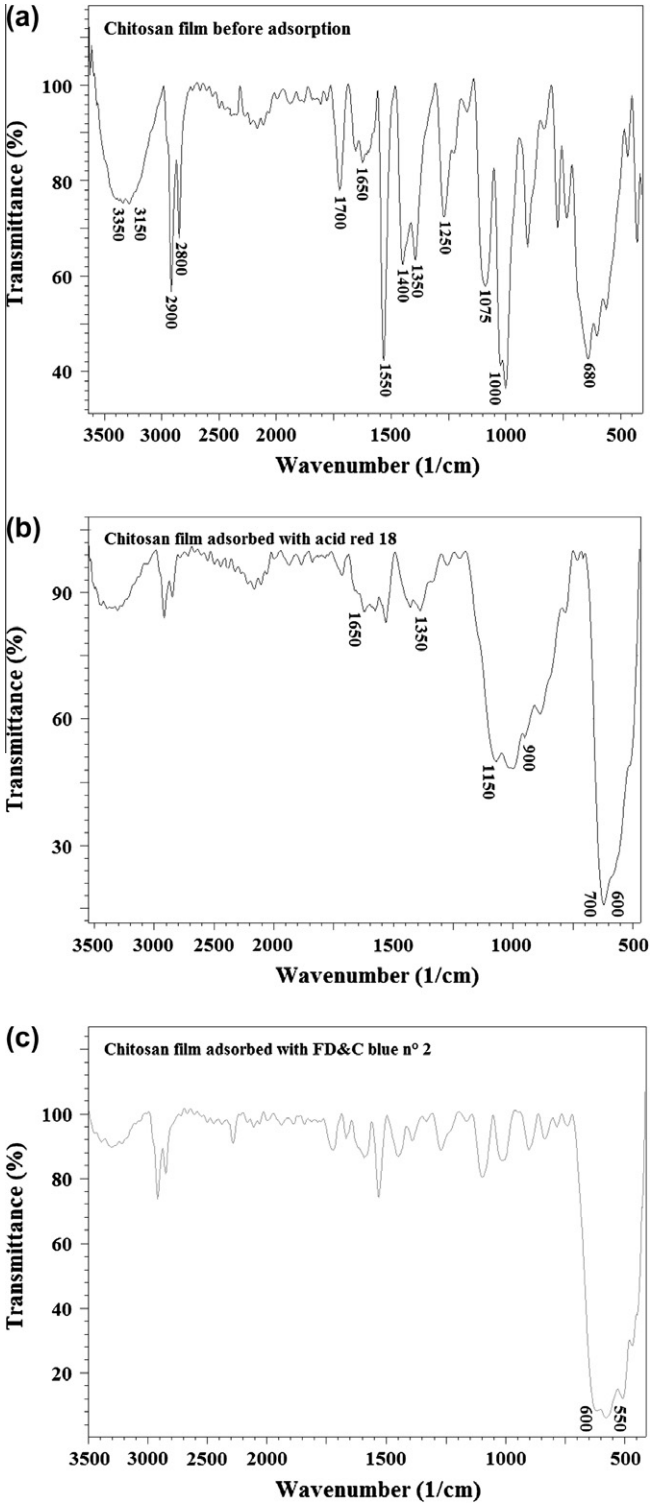

Fig. 5. FT-IR spectrum of chitosan films: (a) before adsorption process, (b) adsorbed with acid red 18, and (c) adsorbed with FD&C blue no. 2.

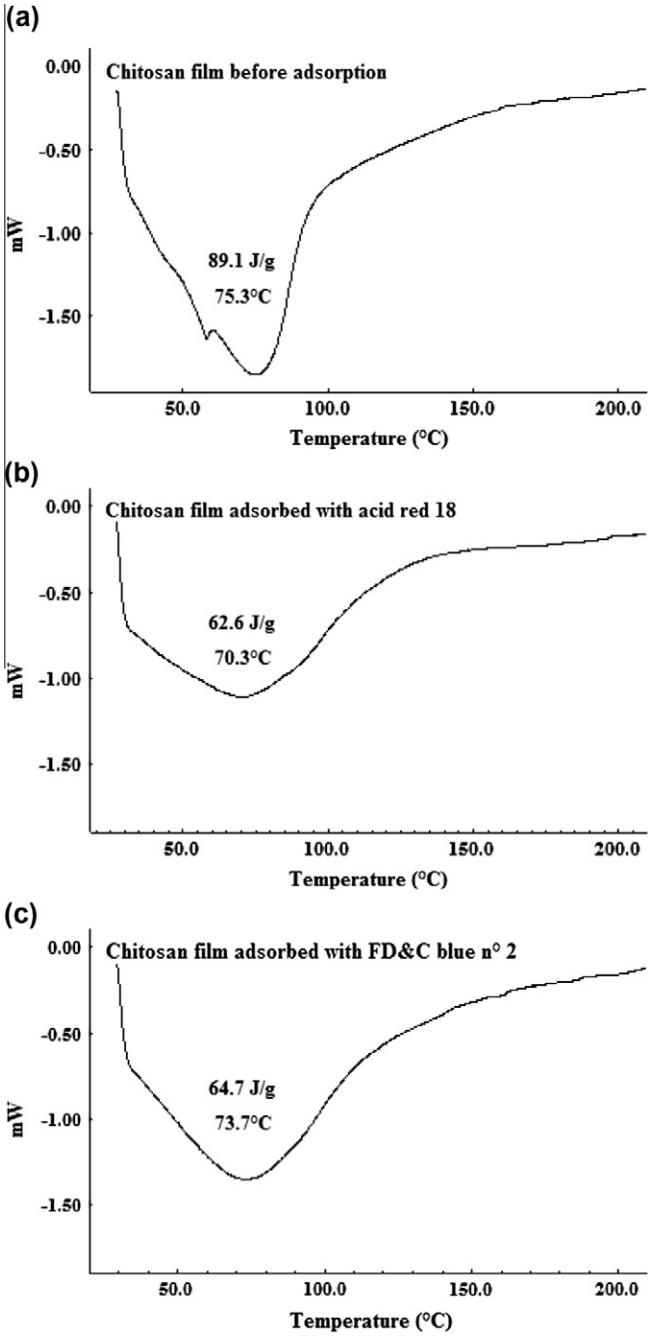

Fig. 6. DSC curves of chitosan films: (a) before adsorption process, (b) adsorbed with acid red 18, and (c) adsorbed with FD&C blue no. 2.

In chitosan films adsorbed with acid red 18 shown in Fig. 5b, carboxilate bands were observed in the range of 1650–1350 cm^{-1}. Furthermore, bending out of plane vibrations, which can be related with substituted aromatic rings, appeared in the range of 1150–900 cm^{-1}. At 700–600 cm^{-1} stretching vibrations of aromatic rings substituted by iodine were identified. This manner, it can be inferred that carboxilate groups and aromatic rings substituted by iodine of the acid red 18 (see Fig. 1a) were involved in the interactions with films. For the chitosan films adsorbed with FD&C blue no. 2 shown in Fig. 5c, bending out of plane vibrations of substituted aromatic rings, and C—S stretching, appeared in the range of 600–550 cm^{-1}. This suggests that the FD&C blue no. 2, the sulfonated groups (see Fig. 1b) were involved in the interactions with chitosan films.

Fig. 6 shows the DSC curves of chitosan films: (a) before adsorption process, (b) adsorbed with acid red 18, and (c) adsorbed with FD&C blue no. 2. Chitosan films before adsorption process showed an endothermic peak at 75.3 °C with enthalpy of 89.1 J g^{-1} (Fig. 6a). This peak could be attributed to evaporation of residual water [27,29]. For the chitosan films adsorbed with acid red 18 (Fig. 5b) and adsorbed with FD&C blue no. 2 (Fig. 6c), the peak was shifted to 70.3 °C (enthalpy of 62.6 J g^{-1}) and 73.7 °C (enthalpy of

Table 5
Color parameters of chitosan films before and after adsorption process.

Color parameters	Chitosan films before adsorption	Chitosan films adsorbed with acid red 18	Chitosan films adsorbed with FD&C blue no. 2
L^*	87.30 ± 0.21	64.52 ± 0.51	29.53 ± 0.32
a^*	0.41 ± 0.13	68.45 ± 0.55	13.61 ± 1.01
b^*	21.85 ± 1.00	6.66 ± 0.34	−27.30 ± 0.75
H_{ab} (°)	88.94 ± 1.05	5.55 ± 0.31	−63.61 ± 1.25

Mean ± standard error (n = 3).

64.7 J g^{-1}), respectively. These shifts show that the interactions between films and water were weakened after adsorption. This occurred due to the migration of large dye molecules (acid red 18 and FD&C blue no. 2) into the polymeric chains of chitosan films.

Table 5 shows the color parameters of chitosan films before and after adsorption process. It can be observed in Table 5 that the L^* value before adsorption was higher than L^* values after adsorption. This shows that the films darkened after the process. Through the H_{ab} values the chitosan films before adsorption showed a faint yellow coloration. After adsorption of acid red 18 and FD&C blue no. 2, the films showed a pink and blue coloration, respectively (see H_{ab} values in Table 5). In summary, these results suggested that the chitosan films were strongly colored during the adsorption of acid red 18 and FD&C blue no. 2, confirming the high affinity between films and food dyes. In addition, chitosan films maintained its structure and were easily separated from the liquid phase after the adsorption process.

Based in FT-IR (Fig. 5), DSC (Fig. 6), color parameters (Table 5) and literature [7–17,43], the following interaction mechanism was proposed for the adsorption of acid red 18 and FD&C blue no. 2 by chitosan films: (1) at neutral pH, about 50% of total chitosan amino groups (NH_2) are protonated (NH_3^+) [7]. So, the cation–cation repulsion occurs, leading to an expansion of chitosan film chains, and favoring the influx of colored liquid into the polymeric network [18]; (2) coupled to this, acid red 18 and FD&C blue no. 2 were dissolved and its groups were dissociated; (3) then, the dyes in anionic form penetrated into films polymeric network (see DSC results) and electrostatic interactions occurred between the negatively charged groups of the dyes (sulfonate or carboxilate) and protonated amino groups of chitosan films (see FT-IR results).

4. Conclusion

In this research, chitosan films were applied to remove food dyes from aqueous solutions. The adsorption capacities of chitosan films were 194.6 mg g^{-1} and 154.8 mg g^{-1} for the acid red 18 and FD&C blue no. 2, respectively, obtained at 298 K. The Redlich–Peterson isotherm model was the more adequate to represent the equilibrium experimental data ($R^2 > 0.98$ and ARE < 9.00%). From the thermodynamic data, it was found that the adsorption of food dyes onto chitosan films is a spontaneous, favorable and exothermic process. The Elovich model was the more appropriate to represent the adsorption kinetic data ($R^2 > 0.95$ and ARE < 5.00%). Electrostatic interactions occurred between the negatively charged groups of the dyes (sulfonate or carboxilate) and protonated amino groups of films. The chitosan films are an alternative to facilitate the phase separation after the dyes adsorption, providing benefits for practical applications.

Acknowledgements

The authors would like to thank CAPES (Brazilian Agency for Improvement of Graduate Personnel) and CNPq (National Council of Science and Technological Development) for the financial support.

References

[1] A. Downham, P. Collins, Coloring our food in the last and next millennium, Int. J. Food Sci. Technol. 35 (2000) 5–22.
[2] N. Koprivanac, H. Kusic, Hazardous Organic Pollutants in Colored Wastewaters, New Science Publishers, New York, 2008.
[3] V.K. Gupta, Suhas, Application of low-cost adsorbents for dye removal: a review, J. Environ. Manage. 90 (2009) 2313–2342.
[4] R.G. Saratale, G.D. Saratale, J.S. Chang, S.P. Govindwar, Bacterial decolorization and degradation of azo dyes: a review, J. Taiwan Inst. Chem. Eng. 42 (2011) 138–157.
[5] A. Srinivasan, T. Viraraghavan, Decolorization of dye wastewaters by biosorbents: a review, J. Environ. Manage. 91 (2010) 1915–1929.
[6] A.K. Verma, R.R. Dash, P.A. Bhunia, A review on chemical coagulation/flocculation technologies for removal of colour from textile wastewaters, J. Environ. Manage. 93 (2012) 154–168.
[7] G. Crini, P.M. Badot, Application of chitosan, a natural aminopolysaccharide, for dye removal from aqueous solutions by adsorption processes using batch studies: a review of recent literature, Prog. Polym. Sci. 33 (2008) 399–447.
[8] W.S. Wan Ngah, L.C. Teong, M.A.K.M. Hanafiah, Adsorption of dyes and heavy metal ions by chitosan composites: a review, Carbohydr. Polym. 83 (2011) 1446–1456.
[9] G.L. Dotto, L.A.A. Pinto, Adsorption of food dyes acid blue 9 and food yellow 3 onto chitosan: stirring rate effect in kinetics and mechanism, J. Hazard. Mater. 187 (2011) 164–170.
[10] G.L. Dotto, L.A.A. Pinto, Adsorption of food dyes onto chitosan: optimization process and kinetic, Carbohydr. Polym. 84 (2011) 231–238.
[11] J.S. Piccin, G.L. Dotto, M.L.G. Vieira, L.A.A. Pinto, Kinetics and mechanism of the food dye FD&C Red no. 40 adsorption onto chitosan, J. Chem. Eng. Data 56 (2011) 3759–3765.
[12] G.L. Dotto, M.L.G. Vieira, L.A.A. Pinto, Kinetics and mechanism of tartrazine adsorption onto chitin and chitosan, Ind. Eng. Chem. Res. 51 (2012) 6862–6868.
[13] J.S. Piccin, M.L.G. Vieira, J.O. Gonçalves, G.L. Dotto, L.A.A. Pinto, Adsorption of FD&C Red No. 40 by chitosan: isotherms analysis, J. Food Eng. 95 (2009) 16–20.
[14] N.M. Mahmoodi, R. Salehi, M. Arami, H. Bahrami, Dye removal from colored textile wastewater using chitosan in binary systems, Desalination 267 (2011) 64–72.
[15] F.C. Wu, R.L. Tseng, R.S. Juang, Characteristics of Elovich equation used for the analysis of adsorption kinetics in dye-chitosan systems, Chem. Eng. J. 150 (2009) 366–373.
[16] L. Fan, C. Luo, X. Li, F. Lu, H. Qiu, M. Sun, Fabrication of novel magnetic chitosan grafted with graphene oxide to enhance adsorption properties for methyl blue, J. Hazard. Mater. 215–216 (2012) 272–279.
[17] A. Mirmohseni, M.S. Seyed Dorraji, A. Figoli, F. Tasselli, Chitosan hollow fibers as effective biosorbent toward dye: preparation and modeling, Bioresour. Technol. 121 (2012) 212–220.
[18] A.R. Fajardo, L.C. Lopes, A.F. Rubira, E.C. Muniz, Development and application of chitosan/poly(vinyl alcohol) films for removal and recovery of Pb(II), Chem. Eng. J. 183 (2012) 253–260.
[19] Y. Tao, L. Ye, J. Pan, Y. Wang, B. Tang, Removal of Pb(II) from aqueous solution on chitosan/TiO_2 hybrid film, J. Hazard. Mater. 161 (2009) 718–722.
[20] A.C.L. Batista, E.R. Villanueva, R.V.S. Amorim, M.T. Tavares, G.M. Campos-Takaki, Chromium (VI) ion adsorption features of chitosan film and its chitosan/zeolite conjugate 13X film, Molecules 16 (2011) 3569–3579.
[21] R.S. Vieira, M.L.M. Oliveira, E. Guibal, E. Rodríguez-Castellón, M.M. Beppu, Copper, mercury and chromium adsorption on natural and crosslinked chitosan films: An XPS investigation of mechanism, Colloids Surf. A: Physicochem. Eng. Aspects 374 (2011) 108–114.
[22] R.F. Weska, J.M. Moura, L.M. Batista, J. Rizzi, L.A.A. Pinto, Optimization of deacetylation in the production of chitosan from shrimp wastes: use of response surface methodology, J. Food Eng. 80 (2007) 749–753.
[23] C.M. Moura, J.M. Moura, N.M. Soares, L.A.A. Pinto, Evaluation of molar weight and deacetylation degree of chitosan during chitin deacetylation reaction: used to produce biofilm, Chem. Eng. Process. 50 (2011) 351–355.
[24] G.L. Dotto, V.C. Souza, L.A.A. Pinto, Drying of chitosan in a spouted bed: the influences of temperature and equipment geometry in powder quality, LWT-Food Sci. Technol. 44 (2011) 1786–1792.
[25] G.L. Dotto, V.C. Souza, J.M. Moura, C.M. Moura, L.A.A. Pinto, Influence of drying techniques on the characteristics of chitosan and the quality of biopolymer films, Drying Technol. 29 (2011) 1784–1791.
[26] American Society for Testing and Materials (ASTM), Standard test Methods for Tensile Properties of Thin Plastic Sheeting (Standard D882–02, 162–170), Philadelphia, 2001.

[27] L.B. Rodrigues, H.F. Leite, M.I. Yoshida, J.B. Saliba, A.S. Cunha Junior, A.A.G. Faraco, In vitro release and characterization of chitosan films as dexamethasone carrier, Int. J. Pharm. 368 (2009) 1–6.
[28] R.M. Silverstein, F.X. Webster, D.J. Kiemle, Spectrometric Identification of Organic Compounds, John Wiley & Sons, New York, 2007.
[29] M. Mucha, A. Pawlak, Thermal analysis of chitosan and its blends, Thermochim. Acta 427 (2005) 69–76.
[30] D.K. Youn, H.K. No, W. Prinyawiwatkul, Physicochemical and functional properties of chitosans affected by sun drying time during decoloration, LWT–Food Sci. Technol. 42 (2009) 1553–1556.
[31] H. Freundlich, Over the adsorption in solution, Z. Phys. Chem. A57 (1906) 358–471.
[32] I. Langmuir, The adsorption of gases on plane surfaces of glass, mica and platinum, J. Am. Chem. Soc. 40 (1918) 1361–1403.
[33] O. Redlich, D.L. Peterson, A useful adsorption isotherm, J. Chem. Phys. 63 (1959) 1024–1027.
[34] M.I. El–Khaiary, G.F. Malash, Common data analysis errors in batch adsorption studies, Hydrometallurgy 105 (2011) 314–320.
[35] Y. Liu, Is the free energy change of adsorption correctly calculated?, J Chem. Eng. Data 54 (2009) 1981–1985.
[36] S.K. Milonjic, A consideration of the correct calculation of thermodynamic parameters of adsorption, J. Serb. Chem. Soc. 72 (2007) 1363–1367.
[37] H. Qiu, L.L. Pan, Q.J. Zhang, W. Zhang, Q. Zhang, Critical review in adsorption kinetic models, J. Zhejiang Univ. Sci. A10 (2009) 716–724.
[38] Y.S. Ho, G. Mckay, Kinetic models for the sorption of dye from aqueous solution by wood, Proc. Safety Environ. Protect. 76 (1998) 183–191.
[39] C.H. Giles, T.H. MacEwan, S.N. Nakhwa, D. Smith, Studies in adsorption part XI: A system of classification of solution adsorption isotherms and its use in diagnosis of adsorption mechanisms and in measurement of specific surface areas of solids, J. Chem. Soc. (1960) 3973–3993.
[40] A.M.M. Vargas, A.L. Cazetta, A.C. Martins, J.C.G. Moraes, E.E. Garcia, G.F. Gauze, W.F. Costa, V.C. Almeida, Kinetic and equilibrium studies: adsorption of food dyes acid yellow 6, acid yellow 23, and acid red 18 on activated carbon from flamboyant pods, Chem. Eng. J. 181–182 (2012) 243–250.
[41] G.L. Dotto, E.C. Lima, L.A.A. Pinto, Biosorption of food dyes onto *Spirulina platensis* nanoparticles: equilibrium isotherm and thermodynamic analysis, Bioresour. Technol. 103 (2012) 123–130.
[42] T.G. Venkatesha, R. Viswanatha, Y.A. Nayaka, B.K. Chethana, Kinetics and thermodynamics of reactive and vat dyes adsorption on MgO mparticles, Chem. Eng. J. 198–199 (2012) 1–10.
[43] J.S. Piccin, G.L. Dotto, L.A.A. Pinto, Adsorption isotherms and thermochemical data of FD&C red no. 40 binding by chitosan, Braz. J. Chem. Eng. 28 (2011) 295–304.